Fine Structure and Physical Properties of Poly(ethylene terephthalate)/Polyethylene Bicomponent Fibers in High-Speed Spinning. II. Poly(ethylene terephthalate) Sheath/Polyethylene Core Fibers

H. H. CHO,[1] K. H. KIM,[1] Y. A. KANG,[1] H. ITO,[2] T. KIKUTANI[2]

[1] Department of Textile Engineering, Pusan National University, Pusan 609-735, Korea

[2] Department of Organic and Polymeric Materials, Tokyo Institute of Technology, 2-12-1, O-Okayama, Meguro-Ku, Tokyo 152, Japan

Received 7 September 1999; accepted 1 December 1999

ABSTRACT: The high-speed melt spinning of sheath/core type bicomponent fibers was performed and the change of fiber structure with increasing take-up velocity was investigated in comparison with the results of our previous study. Two kinds of polyethylene, high density and linear low density (HDPE, LLDPE) with melt flow rates (MFR) of 11 and 50 [HDPE(11), LLDPE(50)], and poly(ethylene terephthalate) (PET) were selected and two sets of sheath/core combinations [PET/HDPE(11) and PET/LLDPE(50) bicomponent fibers] were studied. The structure of each component in high-speed spun bicomponent fibers was analyzed through the birefringence, wide-angle X-ray scattering pattern, differential scanning calorimetry thermogram measurements, tensile tests, and so forth. In the PET/PE bicomponent fiber the structural formation of the PET component was promoted but that of the PE component was suppressed as compared to those of single-component fibers. Neither HDPE nor LLDPE affected the fine structure formation of the bicomponent fiber. Because the thermal properties of PE and PET are quite different from each other, the interfacial instability of the PET/PE bicomponent fiber was found to be serious compared to that of the PE/PET bicomponent fiber. © 2000 John Wiley & Sons, Inc. J Appl Polym Sci 77: 2267–2277, 2000

Key words: polyethylene; poly(ethylene terephthalate); melt spinning; fine structure; physical properties

INTRODUCTION

When two polymers are coextruded as in bicomponent spinning, the stress and thermal histories of each component experienced in the spinline are expected to be significantly different from those in the single-component spinning because of the mutual interaction of the two components. This may also lead to a significant difference in the fiber structure development. Thus, it may be possible to improve the structure of high-speed spun fibers via the choice of suitable component polymers. A clear understanding of the underlying mechanism of structure formation vis-à-vis the processing conditions is however necessary for the effective control of the fiber structure development and thereby the properties of the as-spun fibers.[1–5]

Correspondence to: H. H. Cho.

Journal of Applied Polymer Science, Vol. 77, 2267–2277 (2000)

In our previous study,[6] the sheath/core bicomponent fibers with poly(ethylene terephthalate) (PET) as the core component [i.e., high and linear low density polyethylenes with melt flow rates (MFR) of 11 and 50, respectively, HDPE(11)/PET and LLDPE(50)/PET] were produced by high-speed melt spinning. The structural formation in the spinline during the spinning process and the physical properties of the as-spun fibers at various take-up velocities were investigated, along with those of the single-component fibers.

In the present study the sheath/core bicomponent fibers had PET as the sheath component. The PET/HDPE(11) and PET/LLDPE(50) bicomponent fibers were produced by high-speed spinning and the changes of fiber structure and properties, as well as the interfacial morphology, with the increasing take-up velocity were investigated in comparison with the results of our previous study.

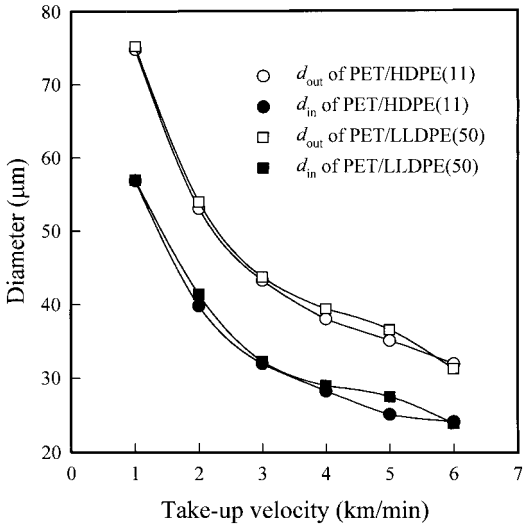

Figure 1 The diameter of PET/PE bicomponent fibers vs. the take-up velocity.

EXPERIMENTAL

High-Speed Spinning of Bicomponent Fiber

We produced sheath/core bicomponent fibers by extruding the melt of general-purpose PET (IV = 0.65 dL/g) as the sheath and PEs (MFR = 11 and 50) as the core through an annular spinneret using two different extrusion systems. Each system consisted of an extruder and a gear pump. The spinning process is the same as that described in a previous article.[6]

Structure and Physical Properties of Fiber

According to the procedure described in our previous article,[6] the birefringence was measured using an interference microscope (Carl-Zeiss Jena) equipped with a polarizing filter and the density was measured at 23°C using a density gradient column. Equatorial X-ray diffraction profiles were obtained by a Rigaku Denki X-ray diffractometer (D/max-III-A type) with an Ni-filtered Cu-Kα radiation source generated at 30 kV and 20 mA. The crystalline orientation was estimated by the azimuthal intensity distribution of well-resolved wide-angle X-ray reflection lines from the (200) and (020) planes of the PE component. The crystalline orientations of the PET components were estimated by the azimuthal intensity distribution from the (100) and (010) planes. The dynamic viscoelastic behavior was investigated using a Rheovibron DDV-II-C (Toyo Baldwin) in a temperature range of 20–200°C at a heating rate of 2°C/min and a frequency of 110 Hz. The thermal behavior of PET/PE bicomponent fibers was investigated using differential scanning calorimetry (DSC, Shimazu DSC-50). DSC measurements were made on 5 mg of the fiber sample, which was cut into small pieces at a heating rate of 20°C/min up to 300°C. The physical properties were tested with a 10-mm length monofilament using a Fafegraph-M tensile tester (Textecho) at a crosshead speed of 20 mm/min. The interfacial morphology between the sheath and core and the existence of voids were confirmed by a polarized microscope (Zeiss) using a mixing refractive liquid with a refractive index similar to that of the PET component in the sheath under a polarized light.

RESULTS AND DISCUSSION

Diameter

Figure 1 shows the diameter of PET/PE as-spun bicomponent fibers as a function of take-up velocity. With increasing take-up velocity the inner and outer radii both decrease gradually. Although a significant difference does not seem to exist between PET/HDPE(11) and PET/LLDPE(50), the diameter of the PET/LLDPE(50) seems to be a little larger than that of PET/HDPE(11) at the take-up velocities covered. This tendency may be

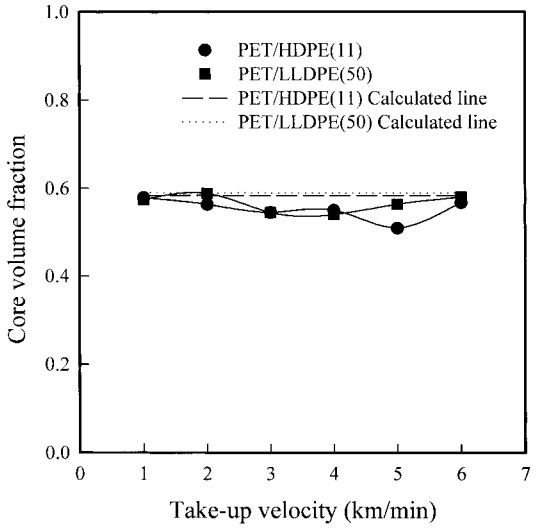

Figure 2 The core volume fraction of PET/PE bicomponent fibers vs. the take-up velocity.

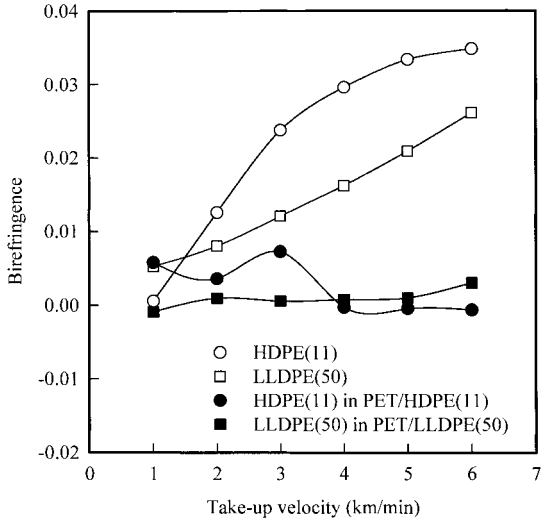

Figure 3 The change of birefringence with take-up velocity for the PE component in PET/PE bicomponent fibers. Birefringences for single-component fibers are also shown for comparison.

because the density of LLDPE is a little smaller than that of HDPE(11). Furthermore, it can be assumed that the spinline tension is almost all concentrated on the PET component as in the PE/PET bicomponent fiber.

Figure 2 shows the change of the core volume fraction with take-up velocity. The dotted lines represent the calculated core volume fraction in which the mass flow rate combination of two components is 1 : 1. It is expected that the spinline is stably independent of the increasing take-up velocity and therefore the sheath and core components can be arranged on a concentric circle.

Molecular Orientation

Figure 3 shows the birefringence of the PE component in the bicomponent fiber as a function of take-up velocity. The birefringence of the PE component is lower at the overall take-up velocities than that of the PE single-component fiber. The birefringence of the PE component is affected by the orientation-induced crystallization of PET. Hence, HDPE(11) with the higher viscosity exhibits the tendency of birefringence to increase up to the take-up velocity of 3 km/min and then decrease. However, the birefringence of LLDPE seems to be close to zero, indicating that the molecular orientation is suppressed as in the PE/PET bicomponent fibers.

Figure 4 shows the birefringence of the PET component in PET/HDPE(11) and PET/LLDPE(50) bicomponent fibers as a function of take-up velocity. Increasing the take-up velocity is supposed to promote the molecular orientation of PET; hence, the birefringence increases remarkably. Above 3 km/min the birefringence of the PET component in PET/LLDPE(50) became slightly larger than that of the PET component of PET/HDPE(11). Judging from the data in Figure 4, the structural formation of the PET component, which experiences higher elongational stress in

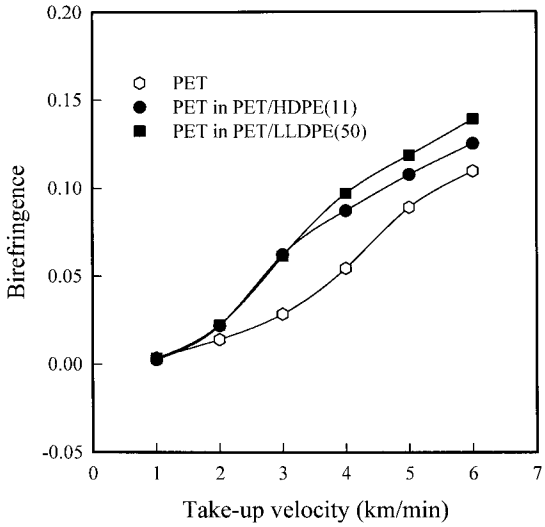

Figure 4 The change of birefringence with take-up velocity for the PET component in PET/PE bicomponent fibers. Birefringences for single-component fibers are also shown for comparison.

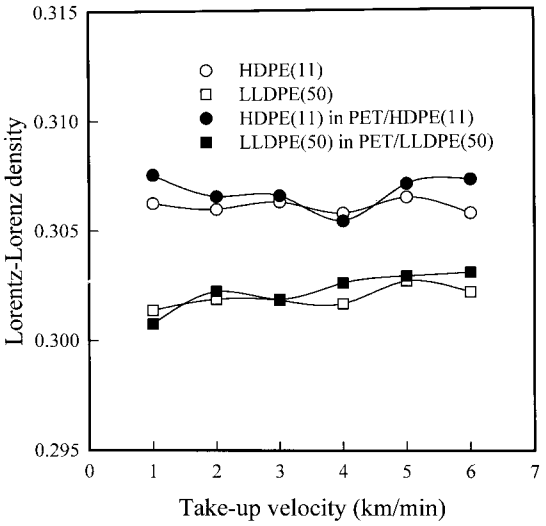

Figure 5 The relation between the Lorentz–Lorenz density and take-up velocity for the PE component in PET/PE bicomponent fibers. The Lorentz–Lorenz densities for a single-component fiber are shown for comparison.

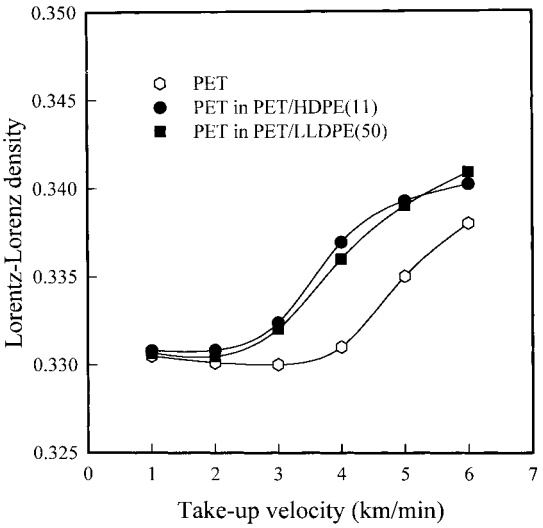

Figure 6 The relation between the Lorentz–Lorenz density and take-up velocity for the PET component in PET/PE bicomponent fibers. The Lorentz–Lorenz densities for a single-component fiber are also shown for comparison.

the spinline, is promoted with increasing take-up velocity, thereby leading to the increase in birefringence. However, we could not find any substantial difference in birefringence between PET/PE and PE/PET bicomponent fibers.

Lorentz–Lorenz Density and Mass Density

The Lorentz–Lorenz densities of the PE component in PET/HDPE(11) and PET/LLDPE(50) bicomponent fibers are plotted as a function of take-up velocity in Figure 5; they exhibit almost a negligible change in the Lorentz–Lorenz density with increasing take-up velocity. The reason for this is that the fraction of the crystalline and amorphous regions is nearly unaffected by the increasing take-up velocity because of the rapid crystallization of the PE component. On the other hand, the difference in the optical density of the PE component between the PET/HDPE(11) and PET/LLDPE(50) may be ascribed to the difference in the respective intrinsic densities.

Figure 6 shows the Lorentz–Lorenz density of the PET component in PET/PE bicomponent fibers as a function of take-up velocity. With increasing take-up velocity the Lorentz–Lorenz density increases; the tendency is remarkable at a take-up velocity of 3–4 km/min, corresponding to the onset of the orientation-induced crystallization.

Figure 7 shows the estimated Lorentz–Lorenz density of a PET/PE bicomponent fiber at the respective take-up velocities, which was calculated by the rule of mixture from the volume fraction of the PE component in the core part. With increasing take-up velocity the packing between the molecular chains is expected to be improved because of the improvement of the orientation.

Figure 8 shows the change of the mass density for PET/PE bicomponent fibers with take-up ve-

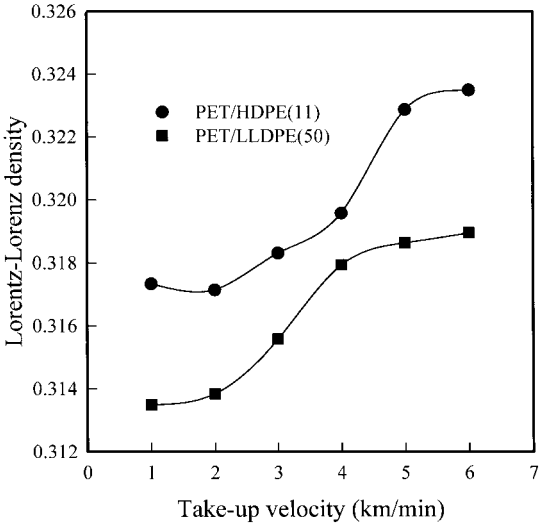

Figure 7 The estimated Lorentz–Lorenz density of PET/PE bicomponent fibers vs. the take-up velocity.

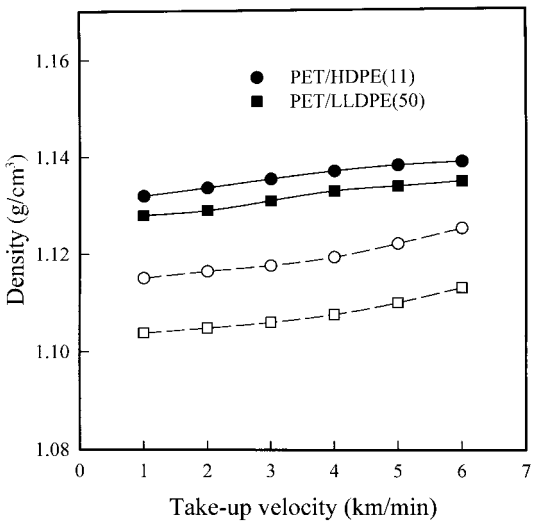

Figure 8 The density of PET/HDPE(11) and PET/LLDPE(50) bicomponent fibers vs. the take-up velocity. (—) The measured density by the density gradient method, and (- - -) the calculated density using the rule of mixture.

locities. The solid lines represent the measured densities by the density gradient method. With increasing take-up velocity the density is gradually increased. The reason is that the density of the PE single-component fiber as shown in our previous results[7,8] remains nearly constant over the take-up velocities covered whereas that of the PET single-component fiber increased because of the orientation-induced crystallization.[9] The dotted lines in Figure 8 represent the density calculated from the rule of mixture using the respective densities of PE and PET spun as a single filament. The difference between the solid and dotted line in the PET/PE bicomponent fiber is larger than that in the PE/PET bicomponent fiber, which was shown in a previous article.[6] This is probably because the orientation of the PET/PE bicomponent fiber is larger. In addition, the PET component in the PET/PE bicomponent fiber may be affected by a shear stress at the spinneret wall.

Figure 9 shows the correlation between the experimental (mass) density in Figure 8 and the Lorentz–Lorenz density calculated from the rule of mixture using the conjugated volume fraction in Figure 7. From this figure a good correlationship is observed like the PE/PET bicomponent fiber. Therefore, by the same argument as our previous results,[6] the packing of the molecular chain for the respective components in the bicomponent fiber was reconfirmed.

Crystalline Structure

Equatorial X-ray diffraction profiles of high-speed spun PET/HDPE(11) and PET/LLDPE(50) bicomponent fibers are shown in Figures 10 and 11, respectively. With increasing take-up velocity, the intensities tend to increase for both cases as in the PE/PET bicomponent fibers. Up to 3 km/min, the reflections from the (110) plane near $2\theta = 22$, the (200) plane near $2\theta = 24.27$, and the (020) plane near $2\theta = 36.8$ were observed for the PE component. This phenomena may be ascribed to the rapid crystallization of PE rather than the effect of orientation-induced crystallization with increasing take-up velocities. At a take-up velocity of 4 km/min, reflections from the (100) plane near $2\theta = 26.4$ and the (010) plane near $2\theta = 17.85$ were observed for the PET component. An increasing take-up velocity causes the peaks to become remarkably sharpened; accordingly, it seems reasonable to say that the orientation-induced crystallization of PET components had progressed. There was no marked difference found in the wide-angle X-ray scattering between the PET/PE and PE/PET bicomponent fibers.

Crystalline Orientation

Figure 12 shows azimuthal diffraction curves of (200) and (020) reflections of the HDPE component in the PET/HDPE(11) bicomponent fiber at various take-up velocities. The (200) plane of crystals for the HDPE component was oriented exclu-

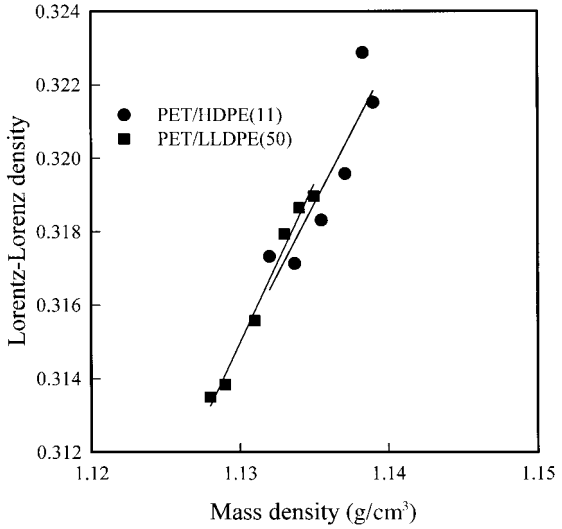

Figure 9 The relation between the mass density and Lorentz–Lorenz density for PET/PE bicomponent fibers.

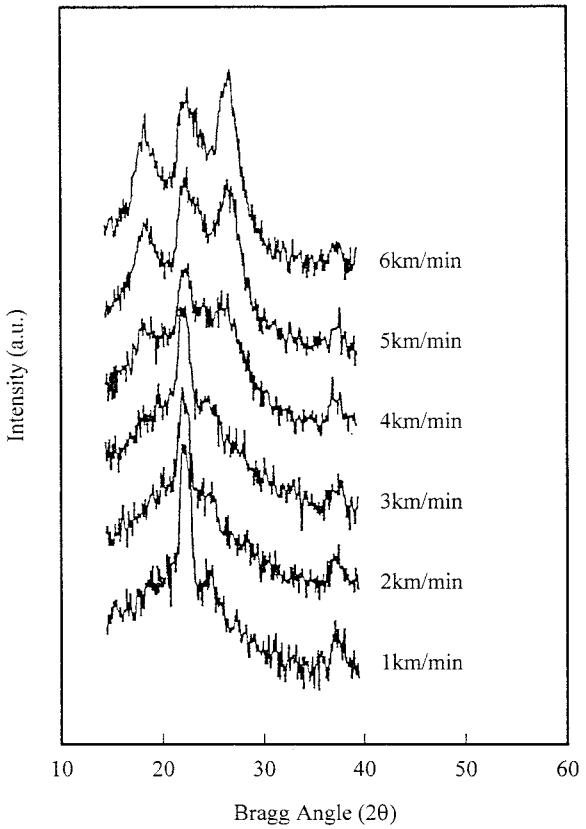

Figure 10 Wide-angle X-ray equatorial scans of PET/HDPE(11) bicomponent fibers vs. the take-up velocity.

sively to the *a*-axis direction up to a take-up velocity of 2 km/min, and above 3 km/min the mixed state of the *a*-axis and *c*-axis orientation was found. This behavior, as in the HDPE(11)/PET bicomponent fiber of our previous study,[6] can be explained by considering the fact that it is mainly concentrated on the PET component.

From Figure 13 for PET/LLDPE(50) bicomponent fiber we can see that the *c*-axis orientation of the PE component seems to be started from a take-up velocity of 2 km/min. With increasing take-up velocity the crystalline orientation likewise increased for the LLDPE(50)/PET in our previous study.[6]

Table I shows the crystalline orientation factor obtained from the azimuthal scans of the (100) and (010) planes of the PET component in PET/HDPE(11) and PET/LLDPE(50) bicomponent fibers. Compared to PET single-component fibers,[7] the crystalline orientation factors of the PET component in bicomponent fibers become somewhat higher with increasing take-up velocity. From this result we again confirmed that the conjugation with PE promotes the crystalline orientation of the PET component.

Dynamic Viscoelasticity

Figure 14 shows the effect of the take-up velocity on the tan δ peaks of the PET/HDPE(11) bicomponent fiber against temperature. On the whole, the curves in Figure 14 mainly reflect the contribution from the amorphous dispersion of the PET component, similar to the HDPE(11)/PET bicomponent fiber. The tan δ peaks tend to shift toward the lower temperature, and the intensities of the tan δ peak decrease with increasing take-up velocity. This tendency suggests that the packing density of the amorphous region in PET is relatively low and the volume of the amorphous region decreases with increasing take-up velocity. Accordingly, this corresponds to the typical tan δ behavior in the PET single-component fiber on high-speed spinning.[9]

Figure 15 shows the tan δ curves of the PET/LLDPE(50) bicomponent fiber, the tendency being similar to Figure 14.

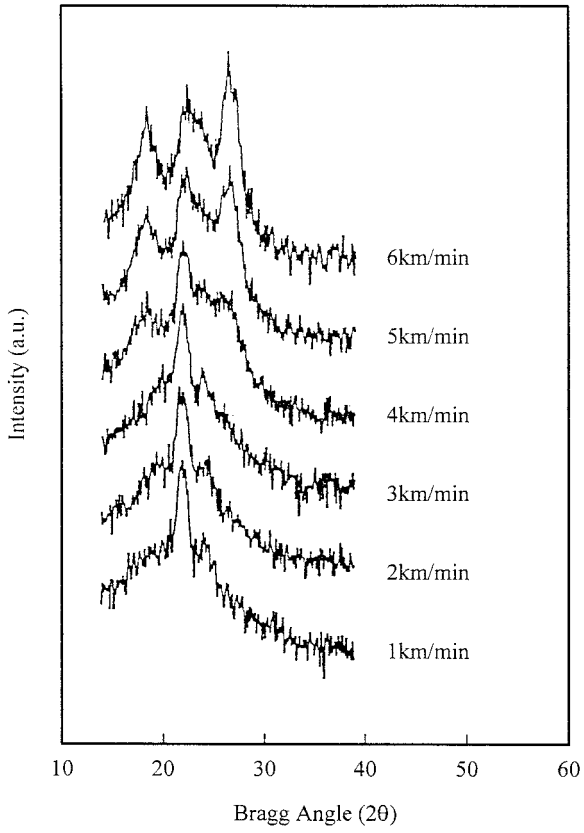

Figure 11 Wide-angle X-ray equatorial scans of PET/LLDPE(50) bicomponent fibers vs. the take-up velocity.

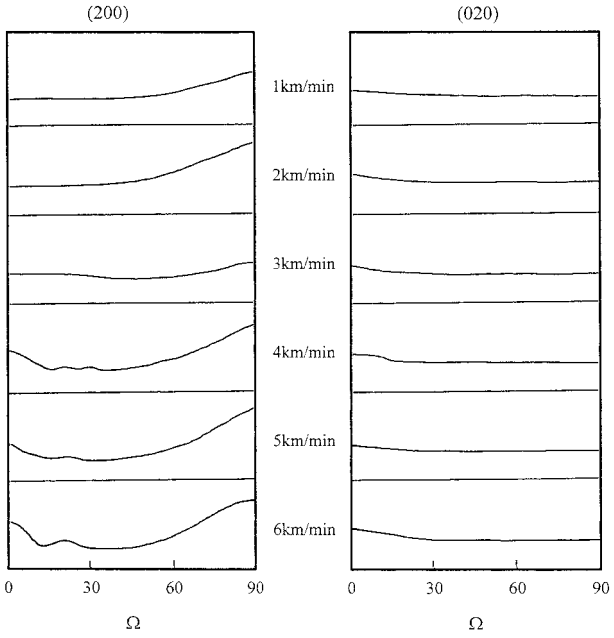

Figure 12 The azimuthal variation of (200) and (020) intensities according to the take-up velocity for the PE component in PET/HDPE(11) bicomponent fibers.

Thermal Behavior

DSC thermograms for the PET/HDPE(11) bicomponent fiber are displayed in Figure 16. This figure shows that in the take-up velocity of 1–2 km/min the solidification and crystallization temperature ($T_{c\ \mathrm{cold}}$) of PET is observed at a temperature just above the melting temperature (T_m) of HDPE; at 2–3 km/min it appears at a temperature just below the T_m of HDPE and finally disappears above a take-up velocity of 4 km/min. This indicates that the orientation-induced crystallization of the PET component in bicomponent fibers is developed more rapidly than the PET single-component fiber, which is in accord with the birefringence results. Above a take-up velocity of 3 km/min, contrary to PE/PET bicomponent fibers, the recrystallization by quenching is expected to occur.[10,11] It may be assumed that the phenomenon of quenching in the PET component is accelerated because the PET component exists in the sheath part, this being subjected to contact because of the surrounding cool air.

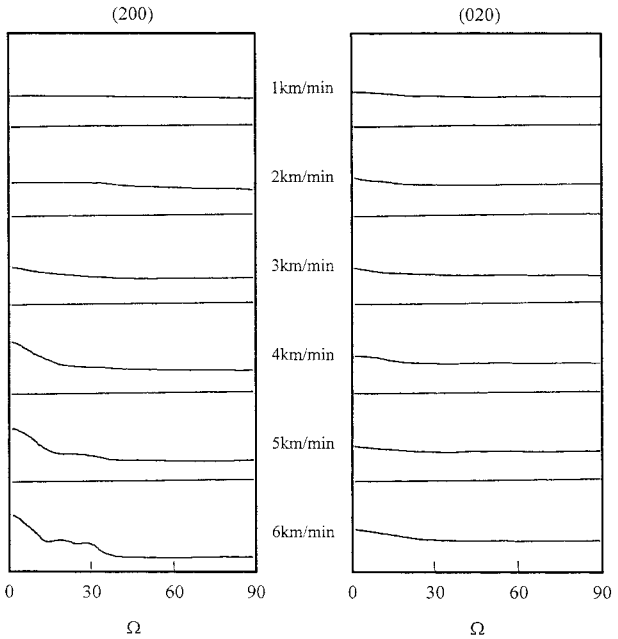

Figure 13 The azimuthal variation of (200) and (020) intensities according to the take-up velocity for the PE component in PET/LLDPE(50) bicomponent fibers.

Table I Crystalline Orientation Factors of PET for Various Fibers with Take-Up Velocities

Sample	Take-Up Velocity		
	4 km/min	5 km/min	6 km/min
PET	0.746	0.895	0.910
PET/HDPE(11)	0.863	0.909	0.922
PET/LLDPE(50)	0.890	0.910	0.923

Figure 17 shows DSC thermograms of PET/LLDPE(50) bicomponent fiber. On the whole, the

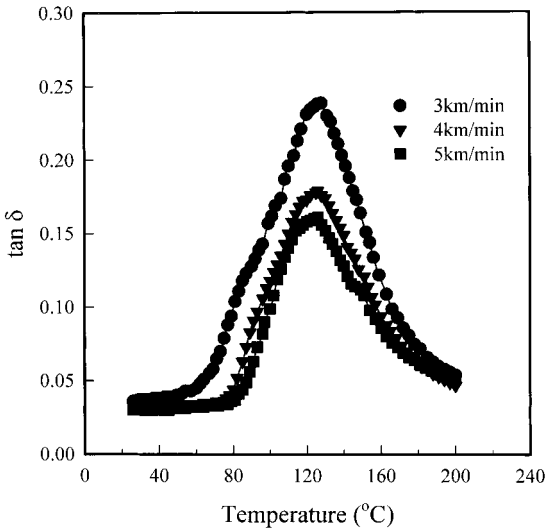

Figure 14 The tan δ vs. temperature for the PET/HDPE(11) as-spun bicomponent fiber at various take-up velocities and 110 Hz.

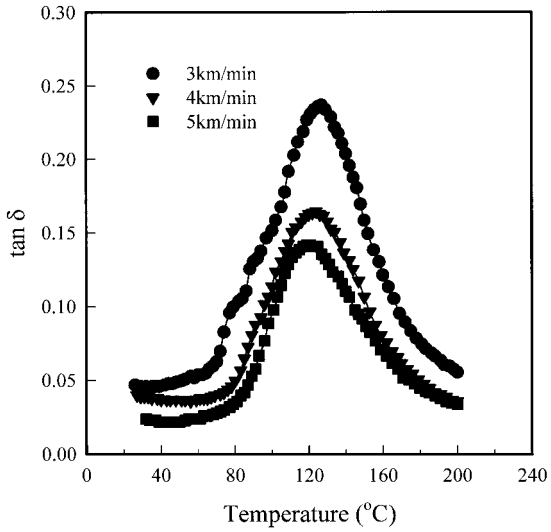

Figure 15 The tan δ vs. temperature for the PET/LLDPE(50) as-spun bicomponent fiber at various take-up velocities and 110 Hz.

$T_{c\ \mathrm{cold}}$ is more clearly observed compared to the PET/HDPE(11) bicomponent fiber in Figure 16, probably because the melting temperature of LLDPE is lower than that of HDPE. The recrystallization peaks of PET are more prominent and the T_m peaks of the PET component are more sharpened than those of the PET/HDPE(11) bicomponent fiber. This may again reflect that the spinline tension during the PET/LLDPE(50) spinning works seriously on the PET component, as stated previously.

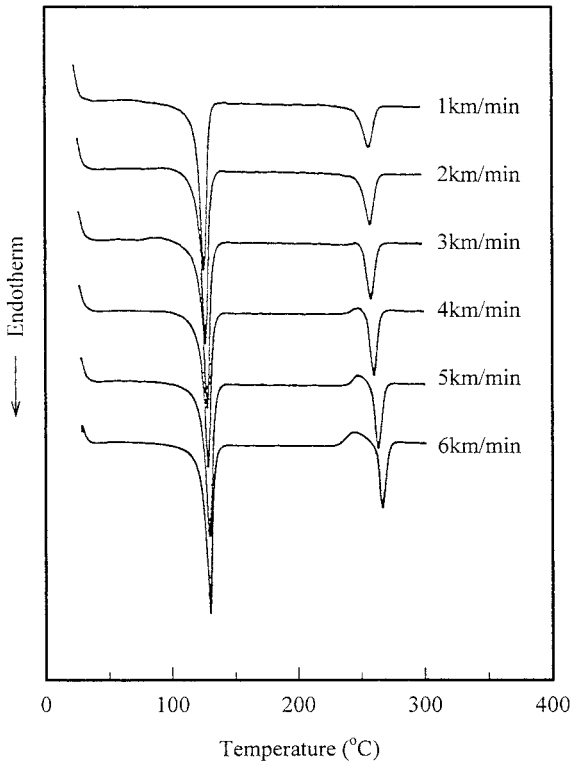

Figure 16 DSC thermograms for PET/HDPE(11) bicomponent fibers obtained at various take-up velocities.

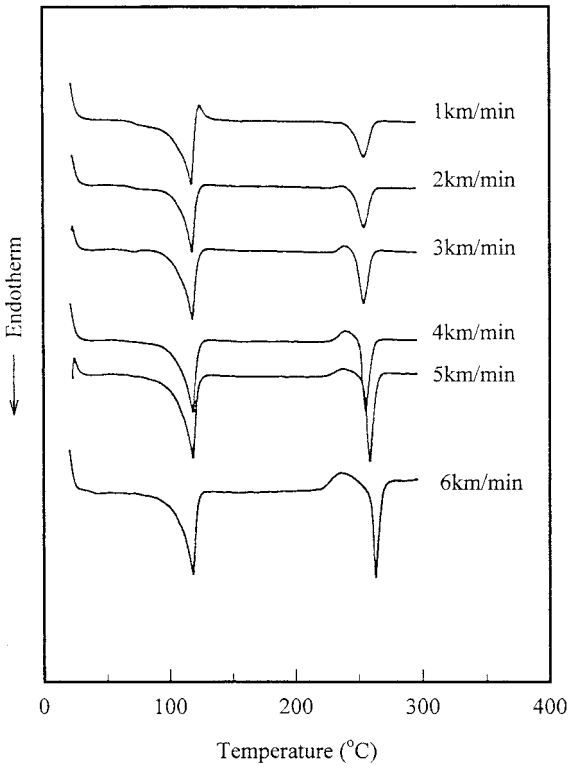

Figure 17 DSC thermograms for PET/LLDPE(50) bicomponent fibers obtained at various take-up velocities.

Tensile Property

Figures 18 and 19 show the stress–strain curves of PET/HDPE(11) and PET/LLDPE(50) bicomponent fibers, respectively, at different take-up velocities. The initial modulus, tenacity, extension, and work of rupture of HDPE(11)/PET, PET/HDPE(11), LLDPE(50)/PET, and PET/LLDPE(50) are shown in Table II for a comparison of physical properties. Increasing the take-up velocity causes the ultimate strain to decrease while the stress and the initial modulus increase. Above the take-up velocity of 3 km/min, the orientation-induced crystallization of PET component is expected to occur. Therefore, the physical properties of as-spun fibers will be sharply increased above the take-up velocity of 3 km/min.

Table II Mechanical Properties of PE/PET and PET/PE Bicomponent Fibers in High-Speed Spinning

Take-Up Velocity (km/min)	Initial Modulus (g/d)				Specific Stress (g/d)				Strain (%)				Work of Rupture (g × cm)			
	HDPE (11)/ PET	PET/ HDPE (11)	LLDPE (50)/ PET	PET/ LLDPE (50)	HDPE (11)/ PET	PET/ HDPE (11)	LLDPE (50)/ PET	PET/ LLDPE (50)	HDPE (11)/ PET	PET/ HDPE (11)	LLDPE (50)/ PET	PET/ LLDPE (50)	HDPE (11)/ PET	PET/ HDPE (11)	LLDPE (50)/ PET	PET/ LLDPE (50)
1	11.61	11.71	11.95	9.61	0.92	0.86	0.72	0.89	638.10	495.08	440.72	520.61	171.32	95.67	147.05	103.95
2	13.26	13.38	13.37	11.48	1.43	1.41	1.46	1.45	329.06	277.05	261.12	276.99	62.39	43.19	88.49	45.57
3	24.43	24.29	20.93	21.06	2.16	1.93	2.31	1.95	141.42	115.56	147.01	121.05	53.73	34.49	56.79	36.56
4	35.00	35.18	31.83	33.08	2.55	2.44	2.58	2.42	92.59	77.25	110.63	72.40	35.73	26.38	42.30	25.10
5	42.88	42.57	40.66	42.83	2.84	2.66	2.82	2.68	83.49	61.07	80.08	55.29	31.29	19.48	29.79	17.85
6	50.22	50.38	48.91	51.76	2.97	2.78	2.95	2.80	68.55	48.12	61.85	42.59	24.23	14.39	22.51	12.81

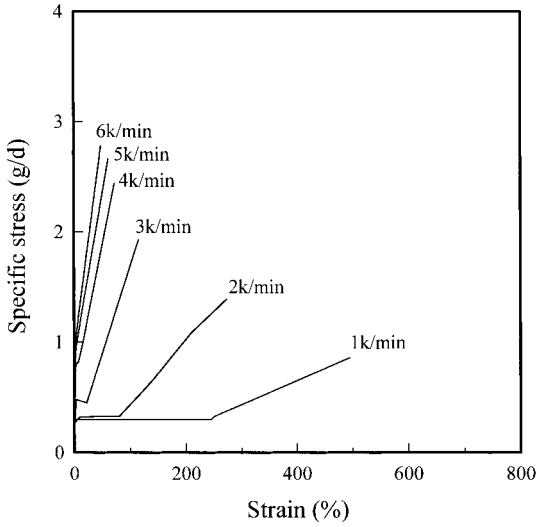

Figure 18 Stress–strain curves of PET/HDPE(11) bicomponent fibers obtained at various take-up velocities.

The physical properties of the PET/PE and PE/PET bicomponent fibers were found to be comparable to each other with increasing take-up velocity. The physical properties of the bicomponent fiber proved to mainly depend on the PET component, which undergoes enhanced structural development by a conjugation with the PE component. No appreciable differences in the physical properties of as-spun bicomponent fibers existed between the combinations of PET/PE and PE/PET: namely, the placement of

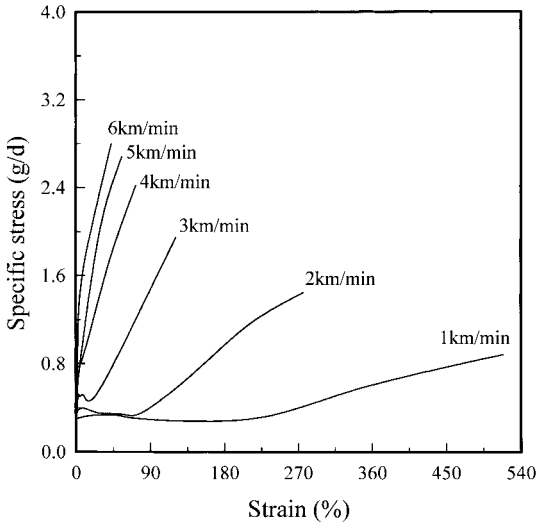

Figure 19 Stress–strain curves of PET/LLDPE(50) bicomponent fibers obtained at various take-up velocities.

Table III Thermal Properties of PE and PET Used for General Purpose

Polymer	Coefficient of Thermal Expansion (mm/mm $K \times 10^6$)	Thermal Conductivity (M/m K)	Specific Heat (kJ/kg K)
HDPE	200	0.38/0.51	2.1/2.7
LDPE	250	0.32/0.40	2.1/2.5
PET	70	0.24	1.05

the PET component in a sheath or core part proved to be of little importance.

Interfacial Morphology

When two polymers are coextruded to form a sheath/core type bicomponent single filament, the stress and thermal histories of each component are expected to be significantly different from those in the single-component spinning because of the mutual interaction of the two components. This may also lead to a significant difference in the fiber structure development. Thus, the thermal properties of PE and PET used for a general purpose are listed in Table III for reference.[12,13] Referring to the data in Table III, it seems reasonable to postulate that the compressional stress in the PE/PET bicomponent fiber will act on the PET component because of the shrinkage force of the PE with a larger thermal expansion coefficient, while in the PET/PE bicomponent fiber phase separation in the interface is expected to occur.

Figure 20 shows the interfacial patterns of PET/HDPE(11) fibers obtained by a polarized microscope. This figure confirms the separation of the interface and the instability at the interface above 3 km/min. In addition, the instability of the interface in PET/HDPE(11) appeared to be more severe than HDPE(11)/PET.

Figure 21 shows the interfacial patterns of PET/LLDPE(50). In LLDPE(50)/PET the separation of interface and the instability in interface were observed above 4 km/min, likewise for LLDPE(50)/PET in a previous study,[6] while in PET/LLDPE(50) the separation at interface and the instability in interface start to be observed from 3 km/min, the tendency being more conspicuous.

Figure 22 illustrates the diameter characterized with a microscope and the diameter calculated from eq. (5) in our companion study for PET/HDPE(11) and PET/LLDPE(50) bicomponent fibers spun at different take-up speeds. No distinct difference between the two diameters was found to exist as in the results of our previous study,[6] suggesting that the density gradient liquid was penetrated in the instability portion of the interface. Consequently, in the combination of PE and PET with negligible miscibility we confirmed that the density gradient liquid fully penetrates into the unstable portion and the interface in the PET/PE bicomponent fiber.

CONCLUSION

High-speed spinning of PET/HDPE(11) and PET/LLDPE(50) bicomponent fibers was car-

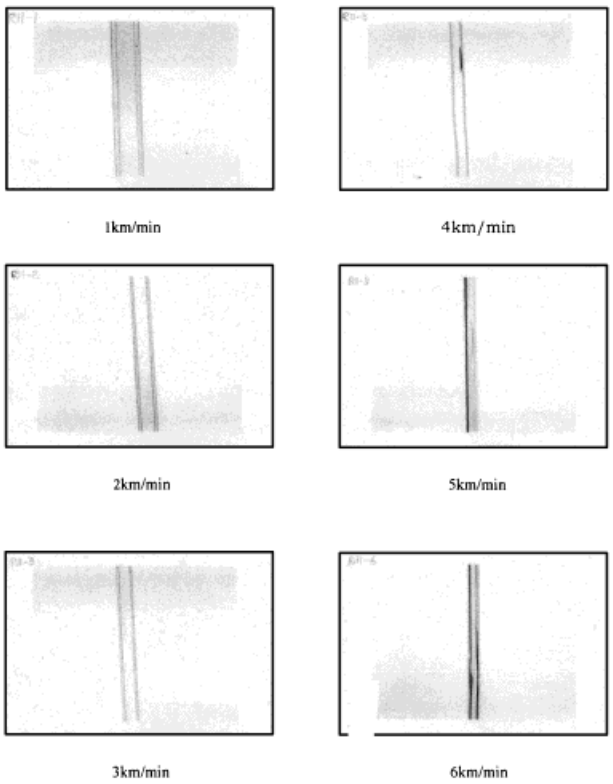

Figure 20 The changes of the interfacial morphology with the take-up velocity for PET/HDPE(11) bicomponent fibers.

ried out, and the fine structure and properties of the fibers spun at various take-up velocities were investigated with birefringence, wide-angle X-ray diffraction, DSC, tensile behavior, and so forth.

1. In the PET/PE bicomponent fiber the structural formation of the PET component was promoted, but that of the PE the component was suppressed compared to those of single-component fibers.
2. Neither HDPE nor LLDPE affected the fine structure formation of the bicomponent fiber.
3. Because the thermal properties of PE and PET are quite different from each other, the interfacial instability of the PET/PE bicomponent fiber was found to be serious compared to that of the PE/PET bicomponent fiber.

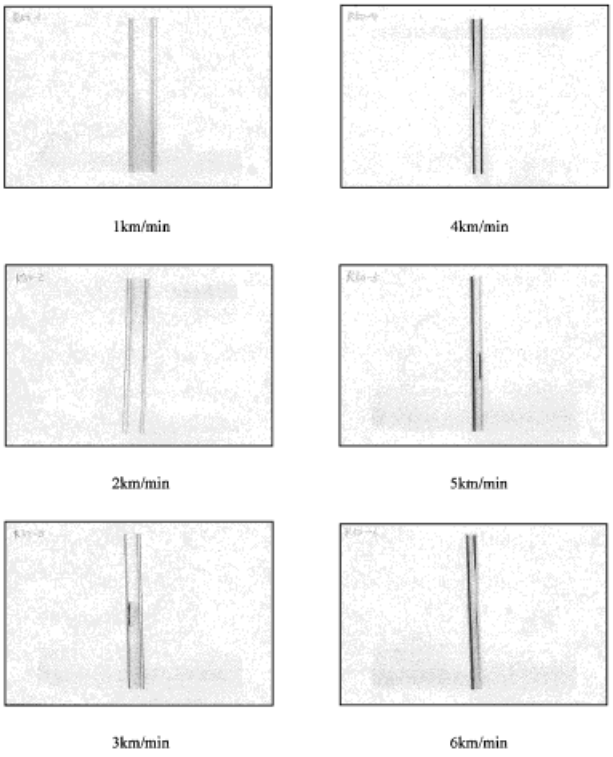

Figure 21 The changes of the interfacial morphology with the take-up velocity for PET/LLDPE(50) bicomponent fibers.

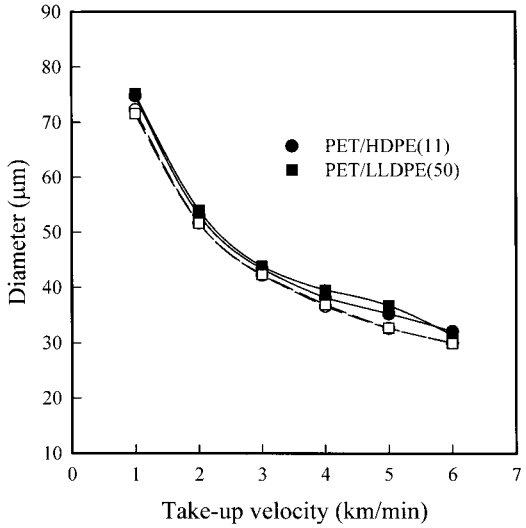

Figure 22 The diameter of PET/PE bicomponent fibers vs. the take-up velocity. (—) The measured diameter by a polarized microscope, and (- - -) the calculated diameter using eq. (5) in our companion study.[6]

REFERENCES

1. Nakajima, T. Advanced Fiber Spinning Technology; Woodhead: Cambridge, U.K., 1994.
2. Kikutani, T.; Radhakrishnan, J.; Arikawa, S.; Takaku, A.; Okui, N.; Jin, X.; Niwa, F.; Kudo, Y. J Appl Polym Sci 1996, 62, 1913.
3. Ziabicki, A.; Kawai, H. High-Speed Fiber Spinning; Wiley: New York, 1985.
4. Ziabicki, A. Fundamentals of Fiber Formation; Wiley: New York, 1976; Chap. 3.
5. Kikutani, T.; Arikawa, S.; Takaku, A.; Okui, N. Sen'i Gakkaishi 1995, 51, 408.
6. Cho, H. H.; Kim, K. H.; Kang, Y. A.; Ito, H.; Kikutani, T. J Appl Polym Sci, to appear.
7. Cho, H. H.; Kim, K. H.; Ito, H.; Kikutani, T. J Appl Polym Sci, to appear.
8. Cho, H. H.; Kim, K. H.; Ito, H.; Kikutani, T. J Appl Polym Sci, to appear.
9. Park, J. B.; Kim, K. H.; Bang, Y. H.; Cho, H. H. J Kor Fiber Soc 1996, 33, 798.
10. Hatakeyama, T. Thermal Analysis: Fundamentals and Applications to Polymers, Wiley: New York, 1994; Chap. 5.
11. Seo, Y. S. Polym Technol 1989, 11, 111.
12. Sperling, L. H. Introduction to Physical Polymer Science; Wiley: New York, 1993; Chap. 8.
13. Progelhof, R. C.; Throne, J. L. Polymer Engineering Principles; Hanser: New York, 1993; Appendix C.